Numerical and Experimental Fracture Analysis of a BWR Pressure Vessel

G. DONZELLA* and L. VERGANI**

*Dipartimento di Meccanica, Universita' di Brescia, Via Valotti 9, 25060 Brescia, Italy

**Dipartimento di Meccanica, Politecnico di Milano, Piazza L.Da Vinci 32, 20133 Milano, Italy

ABSTRACT

A numerical model of a BWR pressure vessel was realized by means of ABAQUS f.e. code and the stress intensity factor KI was calculated for several crack depths. From Paris' law, it was then possible to obtain a prevision crack growth rate.
Experimental measurements on a pressure vessel model, by means of electrical strain gauges and crack gauges, allowed the verification of the numerical model validity and the comparison of the predicted crack growth rate with the experimental one. A good agreement has been shown by this comparison.

KEYWORDS

Fatigue; pressure vessel; multiaxial stress state; stress intensity factor; crack growth; numerical model; crack measurement.

NOTATION

a	crack depth
a_s	calculation crack length on nozzle and vessel inside surfaces
a_n	experimental crack length on the nozzle inside surface
a_v	experimental crack length on the vessel inside surface
a_m	experimental average crack length
E	Young modulus
J	J-integral
K	stress intensity factor
ν	Poisson's elastic ratio
N	cycle number
P	inside pressure
r	crack front radius
r_n	nozzle inside radius
R	vessel inside radius
t	vessel nominal thickness
T	nozzle maximum thickness

INTRODUCTION

During their life period, pressure vessels for light-water nuclear reactors are submitted to a number of cycles of pressurization which is characteristic of the oligocyclic fatigue range. In certain critical areas of the pressure vessel, the junction zone between vessel and nozzles, the local stress greatly exceeds the elastic limit, thus producing serious plastic strains. The repetition of such stress, after a certain number of cycles, causes the formation of a crack which nucleates in the plastic zone, grows into the elastic zone, until it traverses the entire thickness.
A very important parameter for the prediction of the crack propagation rate is the stress intensity factor K_I, here called simply K.
The purpose of this work is to calculate this factor using the f.e.m. and to compare the crack growth prevision so obtained with the experimental one, measured on a pressure vessel model by means of electrical crack gauges.

MECHANICAL MODEL AND EXPERIMENTAL TESTS

A pressure vessel was constructed (Fig.1), fit for testing models of nozzles in scale 1:15, of the same type as those used in the vessels of BWR type nuclear reactor. These nozzles were constructed according to the ASME III Standard Specifications and the vessel was planned to mount three of them, namely A,B,C, at the same time, each at an angle of 120° from each other.
The material used for the construction of the model was type 510 B UNI 7070-82 because it presented a mechanical behaviour which was very similar to that of the material used in the full-scale nozzles. Various specimens were cut from the same bar which was used for the model, and then subjected to tensile tests gave the results reported in Table 1. The stress-strain diagram, obtained from specimens by means of electrical strain gauges, is of the perfectly elasto plastic type, up to an elongation value of 2% . Some electrical strain gauges were pasted to each nozzle, both on the inside and outside surfaces, concentrating them on the vessel-nozzle junction zone.

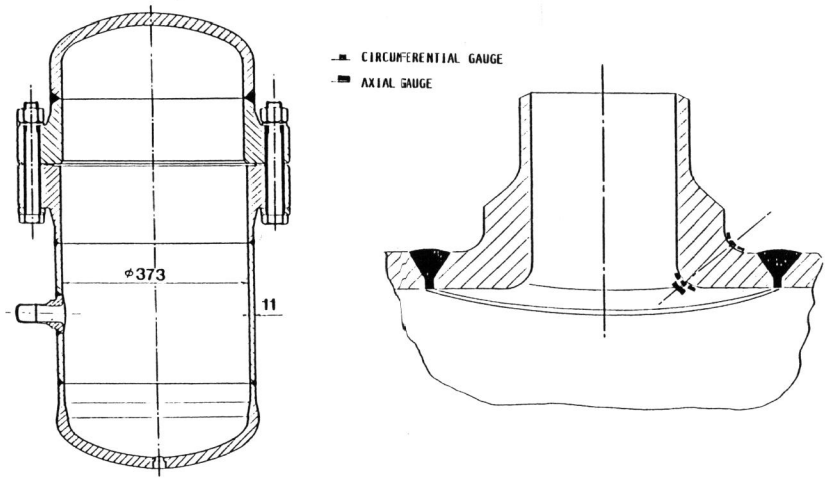

Fig. 1. The vessel model and strain gauges disposal

Table 1. Material properties

Material	yield strengh	tensile strenght	elongation to rupture	Young modulus	Poisson ratio
Fe 510 B	380 MPa	580 MPa	25 %	220000 MPa	0.28

The first experimental test on the vessel was that of a static pressurization, using a hydraulic pump system, up to a pressure of 140 bar. The strain gauge readings, taken at different pressure values, showed a plastic behaviour after p=90 bar in the maximum stress zone: the junction between vessel and nozzle, on the inside surface on the meridian plane of the vessel.

Subsequently, the vessel was submitted to a pulsating pressure P=0÷140 bar, until a through fracture was formed, at different values of load cycles for each of the three nozzles.The strain gauge readings were taken periodically during fatigue testing, to provide information on fatigue crack nucleation, while subsequent propagation was followed by means of electrical crack gauges placed along crack growth directions, towards the nozzle and towards the vessel.

NUMERICAL MODEL

Model without crack

A numerical model was realized by means of the ABAQUS finite element code. A structure was generated which was composed of a quarter of a nozzle, considering the symmetry with respect to the plane passing through the vessel axis and the nozzle axis and with respect to the plane orthogonal to it, and a quarter of the cylindrical shell for such a length on the generatrix so as to reach the stress zone without encountering any interference from the nozzle. The constraints were imposed so as to prevent displacements normal to the plane of symmetry. The loads on the internal surface were indicated as pressure P, while the axial loads corresponding to the internal pressure were applied on the plane which limites the shell structure in the axial direction. The axial stress, corresponding to the aforesaid pressure, was applied on the plane, normal to the nozzle axis, which defines the axial dimension of the nozzle. 144 hexahedral isoparametrical elements of 20 nodes were employed, giving a total node number equal to 917 and 2752 D.O.F. There were two elements lying across the thickness, except for the zone of the junction between vessel and nozzle, while four were placed in circumferential direction. A finer mesh in thickness and circumferential direction did not give significant changes in the results. Two calculations were carried out with this model, one in elastic field, at a pressure of 30 bar, and the other in elasto-plastic field, at a pressure of 140 bar. These numerical results were subsequently compared with the experimental ones.

Model with crack

The cracked model was realized substituting the mesh of the corner zone between vessel and nozzle near the vessel meridian plane, with a refined

crack tip mesh. This model was loaded as the precedent one, with the addition of the pressure load on the free faces of the crack elements.
Six elements were used along the crack front direction, and twelve distribuited radially in four rows of three around the crack tip, so that a focused mesh was produced (Fig.2).

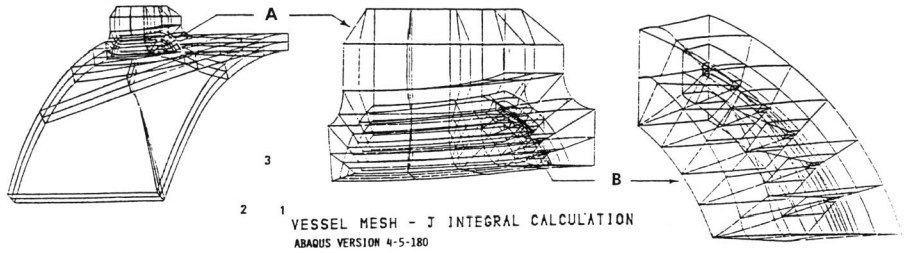

Fig. 2. The mesh for J-integral calculation

196 hexahedral isoparametrical elements of 20 nodes were employed for this cracked mesh, giving a total node number equal to 1322 and 3966 D.O.F.
The mesh was later changed, to consider six different crack depths.
The crack front was taken as circular of radius r and was assumed to grow the same length in every radial direction, so that all different crack fronts were concentric in themselves (see Fig.3).
J integral calculation was carried out in elastic field for every crack depth, at a pressure of 140 bar, using a special procedure of ABAQUS program, based on Parks' virtual crack extension method and was repeated on three different closed contours around the crack tip.

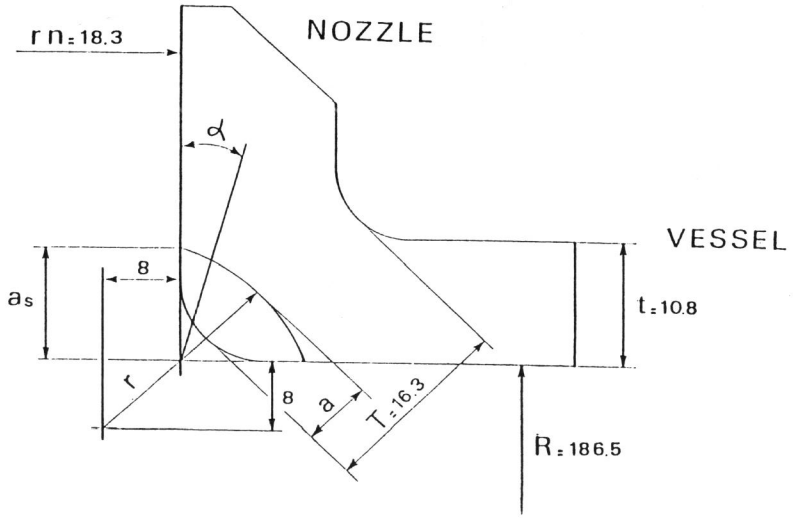

Fig. 3. The crack shape for J-integral calculation

RESULTS

Model without crack, first pressurization

In Fig.4 the distribution of numerical and experimental circumferential strains is indicated, where the origin of the abscissas was placed on the point of maximum curvature of the nozzle inside surface, thus considering the curvature as a straight line and taking the negative direction as that which goes towards the vessel and the positive one as that which goes towards the cylindrical part of the nozzle, to which the piping is welded.
The strains here reported, refer to two different pressurization situations: at 30 bar, in elastic field and at 140 bar, which causes the formation of a plastic zone, of the characteristic elliptic shape, in the maximum stress area. A comparison between experimental and theoretical results, shows a favourable agreement in elastic field, while showing a progressive divergence in plastic field. The average divergence between experimental and numerical results is of 2% at 30 bar, while it reaches the value of 38% at 140 bar.

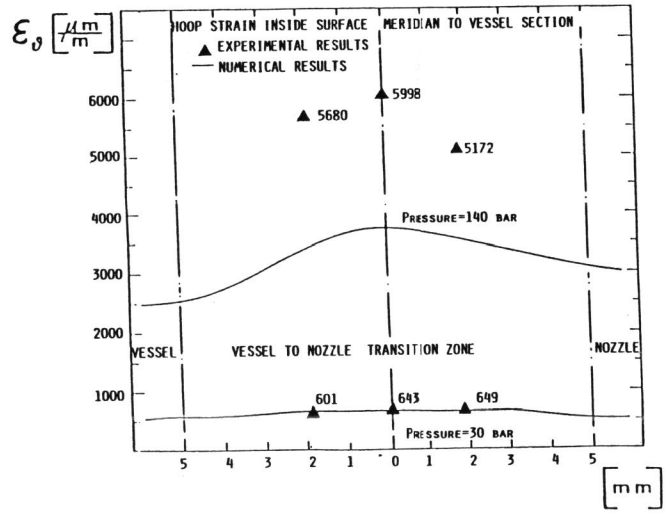

Fig. 4. Numerical and experimental hoop strains

Model with crack, crack propagation rate

The stress intensity factor K was calculated from the J integral, supposing a plane strain condition, from:

$$K^2 = \frac{E \cdot J}{1-\nu^2} \qquad (1)$$

The stress intensity factor distribution along the crack front is reported in Fig.5 for the various crack depths. In this figure K^* is defined as:

$$K^{*}=\frac{K}{P\cdot\sqrt{\pi a^{*}}} \qquad \text{with} \quad a^{*}=6mm \tag{2}$$

It can be seen that the distribution shape changes with the changing of crack depth **a**. More specifically, we note that K is slightly greater towards the nozzle zone ($\alpha=0^{\circ}$) than towards the vessel zone ($\alpha=90^{\circ}$) for small crack depths **a**, while it increases progressively towards the vessel zone with the increasing of crack depths **a**. So, we can suppose that the crack will initially propagate faster in the nozzle direction, while this behaviour will be inverted in the final propagation step.

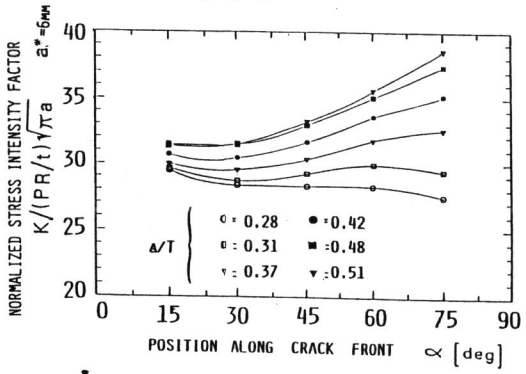

Fig. 5. K^{*} distribution along the crack front

In Fig.6 instead the average normalized stress intensity factor

$$\frac{K}{\frac{P\cdot R}{t}\sqrt{\pi a}} \tag{3}$$

is shown as a function of the normalized crack length a/r_n , where r_n is the nozzle inside radius. In the same figure the results of similar numerical elastic analysis by Gilman & Rashid, Kobayashi et al. and Wilkening, plus an experimental one by Smith, available in literature for comparable nozzle corner flaw geometry, are also plotted.

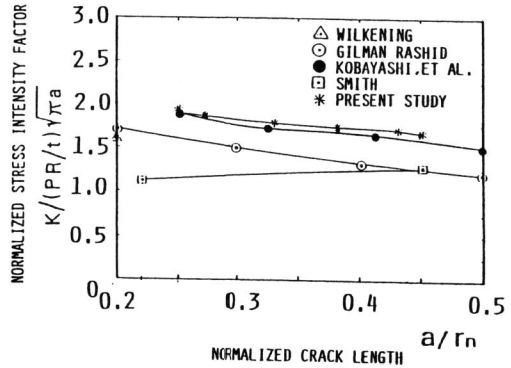

Fig. 6. Normalized K as function of the crack length

In Table 2 the average K values are reported, corresponding to the six crack depths **a** and relative crack size **as** on the free surfaces.

Table 2. Average K values as function of crack depth

a [mm]	4.6	5.0	6.0	6.9	7.9	8.3
as [mm]	9.2	9.7	10.7	11.7	12.7	13.2
K $[MPa\cdot m^{1/2}]$	55.2	56.8	60.1	62.7	65.3	66.4

The comparison with the experimental results is not immediate, due to the scattering of experimental measurements and the simplifications assumed for the numerical calculation. In fact, the crack growth experimentally releaved on nozzles A and B by means of crack gauges, showed different rates in nozzle direction **an** and vessel direction **av** : in nozzle A the crack grew initially faster towards **av** direction and later faster towards **an** direction, while in nozzle B the trend is the opposite (Fig.7).

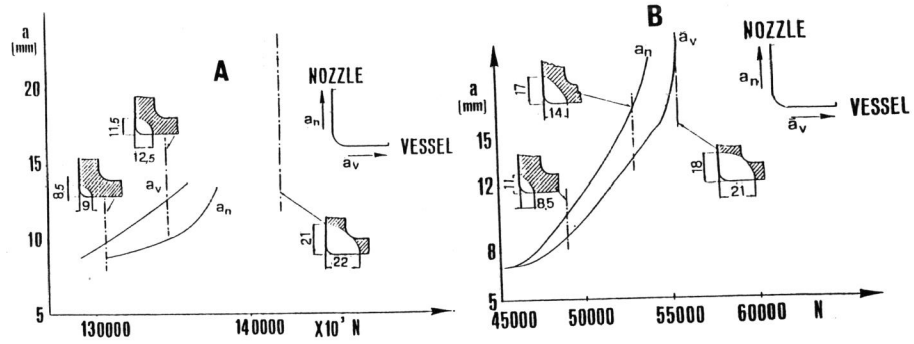

Fig. 7. Experimental crack growth for nozzles A and B

Nozzle B crack propagation shows therefore a qualitative agreement with the numerical K distribution shown in Fig.5. The crack final sizes are however similar on the two nozzle, more specifically slightly wider towards **av** direction.
The average experimental crack growth **am**, calculated as : **am** = (**av** + **an**) versus the cycle number, is reported in Fig.8 for the two nozzles. We can note the different nucleation times, while the propagation ones are similar. From this figure the crack propagation rate $\Delta a/\Delta N$ was calculated in corrispondence with **am** values equal to **as** values assumed for numerical calculation of ΔK.
Corresponding experimental $\Delta a/\Delta N$ and numerical ΔK were plotted in fig.9 in bilogarithmic scale.
In the same figure, Paris' propagation law $\Delta a/\Delta N = C\cdot\Delta K^{n}$, taken from literature for this steel, is shown, with:

$C = 1.6\cdot10^{-12}$ $\quad n = 3.4$ $\quad$ for $\quad \Delta a/\Delta N$ in [m/cycle] and ΔK in $[MPa\cdot\sqrt{m}\,]$

The comparison is substantially favourable: this confirms the validity of the flawed nozzle numerical model.

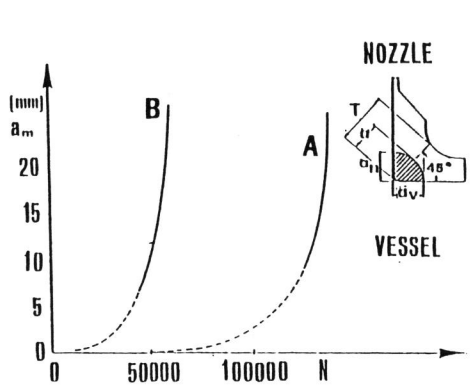

Fig.8. Experimental a_m

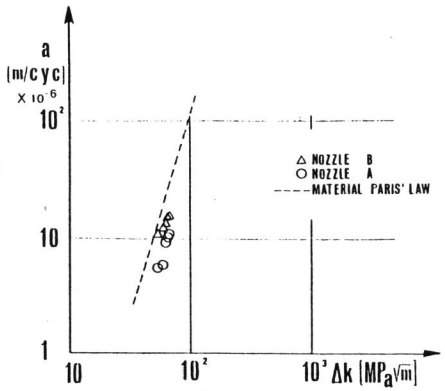

Fig.9. Crack growth prevision

CONCLUSIONS

Numerical calculations and experimental tests were carried out on a BWR pressure vessel model.

- A good agreement was found in elastic field pressurization stress analysis, between numerical and experimental results.
- The flawed numerical model allowed the calculation of the elastic stress intensity factor for six different crack depths: its distribution along the crack front changes with the changing of the crack depth, and its average normalized value versus the normalized crack length results in agreement with recent similar analysis.
- Crack growth was experimentally releaved for two nozzles, allowing the calculation of $\Delta a/\Delta N$. Plotting such experimental $\Delta a/\Delta N$ with numerical ΔK, we found a propagation law very similar to Paris' law of the material.

ACKNOWLEDGEMENTS

This work was supported by the 40% MPI Prof.Bernasconi grant.

REFERENCES

Donzella, G., A. Terranova and L. Vergani.(1987). Crack Nucl. and Propag. in Nozzles of a Pressure Vessel. In: *Low Cycle Fatigue and Elasto-Plastic Behav. of Mat.*(K.T.Rie, ed.),pp 413-418. Elsevier Applied Scienze, London.

Gilman, J. D.(1971). Three-Dimensional Analysis of Reactor Pressure Vessel Nozzles. *1st SMIRT Conference*, Paper G 2/6, Berlin.

Kobayashi,A.,*et al.*(1978). A Procedure for Estimating the S.I.F. of a Flatt. Surface Crack at a Nozzle Corner. *ASME* Paper No.78-PVP-95, Montreal.

Smith, C. W.(1986). Cracking at Nozzle Corners in the Nuclear Pressure Vessel Industry. *ASTM STP 918*, j (C.M.Hudson and T.P.Rich Eds) pp.31-45. American Society for Testing and Materials, Philadelphia.

Wilkening, W. W.(1986). 3-D Elastic Analysis of a Circular Nozzle Corner Crack. *Transaction of the ASME*, 108, 474-478.